Unprecedented trimetallic cluster with an in-plane .mu.3-hydride ligand. X-ray crystal structure of [Mo2(CO)8(.mu.-dppm)(.mu.3-H)(.mu.-AuPPh3)]

Montserrat Ferrer, Roser Reina, Oriol Rossell, Miquel Seco, Santiago Alvarez, Eliseo Ruiz, Maria Angela Pellinghelli, and Antonio Tiripicchio

Organometallics, **1992**, 11 (11), 3753-3759• DOI: 10.1021/om00059a045 • Publication Date (Web): 01 May 2002

Organometallics 1992, *11*, 3753–3759 3753

component of this diminution must be due to the lone pair on arsenic. Previous structural data on lithium cyclenphosphoranide,[2f] Li[cyclenP]

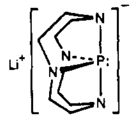

Li[cyclenP]

has shown that the N–P–N equatorial angle is 15–20° smaller than other cyclenPR derivatives. However, the axial N–P–N angle is also decreased, but to a lesser degree, being on the order of 5–10°. There appears to be no such effect on the "axial" angles in HcyclenAs or any of the arsenic species. The arsenic lone pair repulsive effects must be severely diminished with the transannular interaction.

In contrasting HcyclenAs and HcyclenPMo(CO)$_5$, another significant difference is found in the sums of the angles around the nitrogens. The values for $\sum$N(1) and $\sum$N(3) are similar for the two; however, the values for $\sum$N(2) and $\sum$N(4) are 15–20° smaller for arsenic. Previous structural work by Rømming and Songstad[15] has shown very similar structures for trimorpholinophosphine and -arsine [morpholino = N(CH$_2$CH$_2$)$_2$O], where the values for $\sum$N in the arsine are only an average of about 3° lower than in the phosphine. While the smaller bond angles in the arsenic species may be due to the contracted N–As–N equatorial angles, and there is evidence in the data for Li[cyclenP] to support this, it is by no means a general trend.[1f] At this point, the origin of this difference is not clear.

In summary, while there are small differences due to macrocycle ring size and complexation, cyclen and cyclam stabilize pseudo tbp geometries around arsenic, and all three derivatives can be described as zwitterionic arsoranide species. The fact that no As–H bonded derivatives are formed contrasts with the corresponding phosphorus compounds. Since cyclen stabilizes similar geometries around both arsenic and phosphorus, the lack of an As–H bond must be due to its lower thermodynamic stability. In addition, the fact that cyclam stabilizes a pseudo tbp geometry around As in HcyclamAs via a transannular interaction suggests that a similar geometry may exist for the phosphorus open form HcyclamP.

Acknowledgment is made to the Robert A. Welch Foundation and the donors of the Petroleum Research Fund, administered by the American Chemical Society.

Supplementary Material Available: Tables of anisotropic thermal parameters, bond distances, bond angles, and hydrogen atom coordinates and a packing diagram for HcyclenAs showing the chainlike structure (7 pages). Ordering information is given on any current masthead page.

OM920246F

---

[15] Rømming, C.; Songstad, J. *Acta Chem. Scand.* 1980, *A34*, 365.

Unprecedented Trimetallic Cluster with an In-Plane μ_3-Hydride Ligand. X-ray Crystal Structure of [Mo$_2$(CO)$_8$(μ-dppm)(μ_3-H)(μ-AuPPh$_3$)]

Montserrat Ferrer, Roser Reina, Oriol Rossell,* Miquel Seco, Santiago Alvarez,* and Eliseo Ruiz

Departament de Química Inorgànica, Universitat de Barcelona, Diagonal 647, 08028 Barcelona, Spain

Maria Angela Pellinghelli and Antonio Tiripicchio*

Istituto di Chimica Generale ed Inorganica, Università di Parma, Centro di Studio
per la Strutturistica Diffrattometrica del CNR, Viale delle Scienze 78, 43100 Parma, Italy

Received March 16, 1992

The salt (NEt$_4$)[Mo$_2$(CO)$_8$(μ-dppm)(μ-H)] [dppm = bis(diphenylphosphino)methane] reacts with XMPPh$_3$ (M = Au, Cu, Ag; X = Cl, I) in tetrahydrofuran to yield [Mo$_2$(CO)$_8$(μ-dppm)(μ_3-H)(μ-MPPh$_3$)] (M = Au, **1a**; M = Ag, **1b**; M = Cu, **1c**). The structure of **1a** has been determined by X-ray diffraction methods. Crystals are orthorhombic, space group $P2_12_12_1$ with $Z = 4$ in a unit cell of dimensions a = 12.361 (5), b = 15.179 (6), and c = 25.800 (8) Å. The structure has been solved from diffractometer data by direct and Fourier methods and refined by full-matrix least-squares on the basis of 2309 observed reflections to R and R_w values of 0.0504 and 0.0668, respectively. The structure of **1a** is without precedent in that the metal core, consisting of an almost symmetric Mo$_2$Au triangular framework, is held by a hydride ligand located in the same plane defined by the metal atoms. Although an accurate location of this hydride was not possible, there are several lines of evidence in agreement with this position. The Mo–Mo separation is 3.771 (3) Å, and the Mo–Au bond lengths are 2.900 (3) and 2.914 (2) Å. Reaction of (NEt$_4$)[Mo$_2$(CO)$_8$(μ-dppm)(μ-H)] with (ClAu)$_2$(μ-PP) (PP = dppm, dppe [1,2-bis(diphenylphosphino)ethane], and dppp [1,3-bis(diphenylphosphino)propane]) leads to the hexametallic complexes [{Mo$_2$(CO)$_8$(μ-dppm)(μ_3-H)(μ-Au)}$_2$(PP)] (PP = dppm, **2a**; PP = dppe, **2b**; PP = dppp, **2c**), which contain two metal cluster fragments linked by a bridging diphosphine. The bonding within the Mo$_2$HAu skeleton and the structural differences between **1a** and the parent anion [Mo$_2$(CO)$_8$(μ-dppm)(μ-H)]$^-$ are explained on the basis of molecular orbital calculations.

Introduction

The synthesis, structural characterization, and reactivity study of gold hydride species is a rapidly expanding area because of their potential use in the field of homogeneous and heterogeneous bimetallic catalysis.[1] Although mononometallic gold hydride compounds have not been directly observed, several heterobimetallic complexes are known in which a hydride ligand bridges a transition metal and

---

[1] Braunstein, P.; Rosé, J. *Gold. Bull.* 1985, *18*, 17.

0276-7333/92/2311-3753$03.00/0 © 1992 American Chemical Society

a gold atom. The most important route for the synthesis of such species is the reaction of $Au(PPh_3)^+$ with metal hydride complexes. For example, by means of this synthetic procedure, Venanzi and co-workers in their pioneering work[2] reported the complexes $[(PPh_3)_3(H)_2Ir(\mu\text{-}H)(AuPPh_3)]BF_4$ and $[(PEt_3)_2(C_6Cl_5)Pt(\mu\text{-}H)(AuPEt_3)]BF_4$. Simultaneously, Stone et al. isolated several neutral complexes of the type $[(OC)_5M(\mu\text{-}H)(AuPR_3)]$ (M = Cr, Mo, W; R = Et, Ph),[3] and the number of bimetallic species has been increasing during recent years.[4] Moreover, several hydride derivatives containing more than one gold atom have been also described and listed in the excellent review of Pignolet.[5] Although no orbital molecular calculations have been carried out on this type of compound, it has been suggested that the primary interaction between a transition-metal hydride and a gold(I) phosphine fragment is the donation of the two electrons contained in the metal–hydride bond into the empty gold(I) sp_z hybrid orbital.[6] However, it has also been noted that the relatively short metal–metal bond distances found in some cases do not rule out significant metal–gold bonding, through the interaction of an empty gold p orbital and a filled component of the "t_{2g}" remnants of the heteroatom.[6,7]

Following our studies on mixed gold–transition-metal clusters[8–10] and with the object of gaining insight into the nature of bonding in hydride–transition-metal systems, we have undertaken a study involving the molybdenum complex $[Mo_2(CO)_8(\mu\text{-dppm})(\mu\text{-}H)]^-$ [dppm = bis(diphenylphosphino)methane] as a donor species. Since this compound features a hydride bridging two molybdenum atoms,[11] we considered that it might be suitable for giving, after reaction with the electrophilic $AuPPh_3^+$ moiety, a three metal system held by a hydride in a μ_3 bonding mode. This idea is supported by orbital molecular calculations on the electronic structure of the molybdenum derivative which indicate that high electronic density is located on the hydride (see below). In this paper we report the synthesis of the neutral complexes $[Mo_2(CO)_8(\mu\text{-dppm})(\mu_3\text{-}H)(\mu\text{-}MPPh_3)]$ (M = Cu, Ag, Au), the X-ray crystal structure of the gold compound, and three new derivatives in which two Mo_2Au units are linked by a bridging ligand as a result of our unsuccessful attempts to promote condensation reactions between the two cluster fragments. Finally, the bonding in the Mo_2HAu core is described in terms of a delocalized molecular orbitals, on the basis of the results of extended Hückel calculations.

Results and Discussion

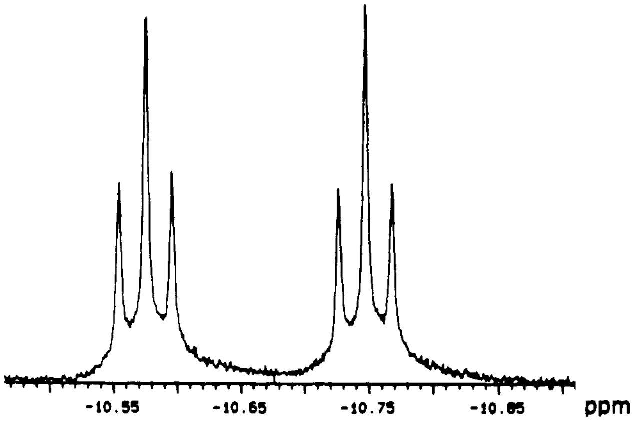

Figure 1. ^1H NMR spectrum of **1a** in the hydride region.

Upon treatment of the dimolybdenum hydride salt $(NEt_4)[Mo_2(CO)_8(\mu\text{-dppm})(\mu\text{-}H)]$ with $ClAuPPh_3$ in the presence of $TlBF_4$, in tetrahydrofuran solution (−20 °C), the compound $[Mo_2(CO)_8(\mu\text{-dppm})(\mu_3\text{-}H)(\mu\text{-}AuPPh_3)]$ (**1a**) is isolated in high yield according to eq 1. **1a** is an air-stable yellow solid, but its solutions decompose slowly when allowed to warm to room temperature. Copper and silver compounds $[Mo_2(CO)_8(\mu\text{-dppm})(\mu_3\text{-}H)(\mu\text{-}MPPh_3)]$ (M = Ag, **1b**; M = Cu, **1c**) were similarly prepared from the molybdenum anion and $IMPPh_3$ and showed analogous stability. Compounds **1a–c** were characterized by elemental analyses and spectroscopic techniques. The IR spectra showed an identical pattern in the ν(CO) region for the three compounds, and the ν(CO) bands shifted slightly to higher frequencies with respect to the molybdenum anion, suggesting a decrease of electron density on the molybdenum atoms. On the other hand, no peaks in the terminal hydride stretching region (1700–2300 cm^{-1}) were observed and unfortunately the bridging region (800–1400 cm^{-1}) is complicated by many intense absorptions of the ligands. The low-temperature ^{31}P NMR spectra of **1a–c** in THF solutions are consistent with the solid-state structure. Thus, the $AuPPh_3$ signal appears as a triplet, while the MoP peaks appear as a doublet, as expected for an AX_2 type spectrum. For **1b** it was not possible to determinate either $^2J(P\text{-}^{107}Ag)$ and $^2J(P\text{-}^{109}Ag)$ or $^3J(P\text{-}P)$ since broad peaks were observed for both types of phosphorus atoms. From these spectra it is deduced that the bridging nature of diphosphine is retained in the new complexes. The ^1H NMR spectra are more informative and show unambigously the symmetric trimetallic nature of the compounds with the hydride bonded to the three metals. Thus, in the hydride region, the spectrum of **1a** (Figure 1) displays a doublet of triplets, the coupling constant in the (μ-H)$AuPPh_3$ unit (85.9 Hz) being similar to those found in $[(CO)_5Cr(\mu\text{-}H)(AuPPh_3)]$[3] (105 Hz) and $[(PPh_3)_3H_2Ir(\mu\text{-}H)(AuPPh_3)]BF_4$[2] (79.4 Hz), and confirms the transoid H–Au–PPh$_3$ arrangement. Interestingly the NMR spectra are not temperature-dependent, indicating that no dynamic behavior occurs, in clear contrast with the recent reports on hydride gold–ruthenium clusters.[12]

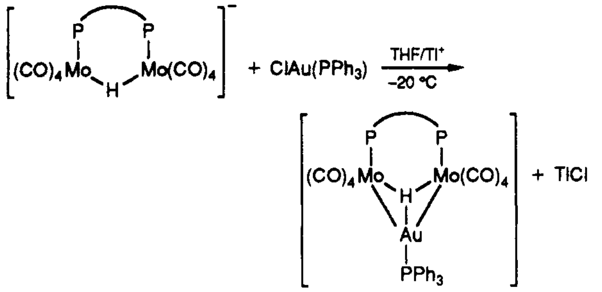

(1)

---

[2] Lehner, H.; Matt, D.; Pregosin, P. S.; Venanzi, L. M. *J. Am. Chem. Soc.* **1982**, *104*, 6825.

[3] Green, M.; Orpen, A. G.; Salter, I. D.; Stone, F. G. A. *J. Chem. Soc., Chem. Commun.* **1982**, 813.

[4] (a) Albinati, A.; Lehner, H.; Venanzi, L. M. *Inorg. Chem.* **1987**, *26*, 3933. (b) Crespo, M.; Sales, J.; Solans, X. *J. Chem. Soc., Dalton Trans.* **1989**, 1089.

[5] Mueting, A. M.; Bos, W.; Alexander, B. D.; Boyle, P. D.; Casalnuovo, J. A.; Balaban, S.; Ito, L. N.; Johnson, S. M.; Pignolet, L. H. *New J. Chem.* **1988**, *12*, 505.

[6] Albinati, A.; Demartin, F.; Janser, P.; Rhodes, L. F.; Venanzi, L. M. *J. Am. Chem. Soc.* **1989**, *111*, 2115.

[7] Freeman, M. J.; Orpen, A. G.; Salter, I. D. *J. Chem. Soc., Dalton Trans.* **1987**, 379.

[8] Rossell, O.; Seco, M.; Jones, P. G. *Inorg. Chem.* **1990**, *29*, 348.

[9] Reina, R.; Rossell, O.; Seco, M.; Ros, J.; Yáñez, R.; Perales, A. *Inorg. Chem.* **1991**, *30*, 3973.

[10] Alvarez, S.; Rossell, O.; Seco, M.; Valls, J.; Pellinghelli, M. A.; Tiripicchio, A. *Organometallics* **1991**, *10*, 2309.

[11] Darensbourg, M. Y.; El Mehdawi, R.; Delord, T. J.; Fronczek, F. R.; Watkins, S. F. *J. Am. Chem. Soc.* **1984**, *106*, 2583 and references therein for other related Mo–H–Mo systems.

It seemed of interest to extend the synthetic approach for **1a–c** to the compounds $[Mo_2(CO)_8(\mu\text{-dppp})(\mu_3\text{-H})(\mu\text{-MPPh}_3)]$ [dppp = 1,3-bis(diphenylphosphino)propane] in order to study the influence of the steric strain caused by the presence of three CH_2 units in the diphosphine chain on the final stability of the products. When the compound $(NEt_4)[Mo_2(CO)_8(\mu\text{-dppp})(\mu\text{-H})]$ was reacted in THF solution (−70 °C) with $ClAuPPh_3$, in the presence of $TlBF_4$, the solution became yellow-orange. After filtration of the salts, the ^{31}P NMR spectrum displayed three signals at 49.1 (P_A), 34.2 (P_B), and 27.8 (P_C) ppm with $J(P_A–P_B)$ = 7.0 Hz, strongly suggesting the formation of the species **3**.

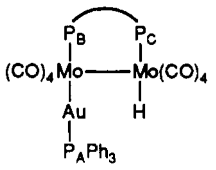

3

Considering a Mo–Mo bond, this compound would attain the 18-electron configuration. Unfortunately, we were not able to isolate the complex since during the process of solvent evaporation, it rapidly began to decompose. For this, we could not run the ^1H NMR spectrum that would have been very informative. In a first approach, the high instability of this complex is understood on the basis of the presumably long Mo–Mo separation in the starting anion (this has been found to be 3.403 (1) Å with the $Ph_2P(CH_2)PPh_2$ ligand and 3.499 (1) Å with the $Ph_2P(CH_2)_4PPh_2$ ligand),[11] which would disfavor the formation of the μ_3-hydride triangular metal cluster. Similar results have been recently found for mercury–molybdenum metal–metal-bonded complexes.[13]

In order to investigate the possibility of promoting condensation reactions to give heteropolynuclear clusters between two Mo_2Au units, we allowed the salt $(NEt_4)[Mo_2(CO)_8(\mu\text{-dppm})(\mu\text{-H})]$ to react with $(ClAu)_2(\mu\text{-P}'\text{-P}')$ (P′-P′ = dppm, dppe [1,2-bis(diphenylphosphino)ethane], and dppp) in tetrahydrofuran. In all cases the species obtained were the hexametallic complexes containing two Mo_2Au units bridged by a diphosphine ligand (eq 2).

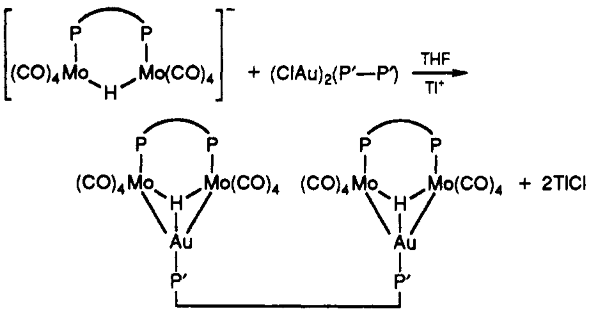

(2)

P′—P′ = dppm (**2a**)
P′—P′ = dppe (**2b**)
P′—P′ = dppp (**2c**)

Complexes **2a–c** were formulated on the basis of elemental analyses and IR and NMR spectroscopy. The species reported here are very close to those recently reported containing symmetric or asymmetric Fe_2Au units,[8,9] and we believe that the high thermodynamic stability of the Mo_2Au or Fe_2Au metal systems precludes the synthesis of species with higher nuclearity.

Table I. Selected Bond Distances (Å) and Angles (deg) with Esd's in Parentheses for Compound 1a

Au–Mo(1)	2.900 (3)	P(2)–C(28)	1.81 (3)
Au–Mo(2)	2.914 (2)	P(2)–C(34)	1.82 (3)
Au–P(1)	2.286 (7)	P(3)–C(9)	1.83 (3)
Mo(1)–P(2)	2.530 (7)	P(3)–C(40)	1.87 (3)
Mo(1)–C(1)	1.94 (3)	P(3)–C(46)	1.85 (3)
Mo(1)–C(2)	1.84 (3)	C(1)–O(1)	1.20 (4)
Mo(1)–C(3)	2.04 (2)	C(2)–O(2)	1.25 (4)
Mo(1)–C(4)	2.03 (3)	C(3)–O(3)	1.12 (3)
Mo(2)–P(3)	2.557 (7)	C(4)–O(4)	1.16 (4)
Mo(2)–C(5)	1.95 (2)	C(5)–O(5)	1.15 (3)
Mo(2)–C(6)	1.95 (3)	C(6)–O(6)	1.15 (4)
Mo(2)–C(7)	2.03 (3)	C(7)–O(7)	1.11 (3)
Mo(2)–C(8)	2.03 (3)	C(8)–O(8)	1.12 (5)
P(1)–C(10)	1.84 (3)	Au–H(1)	1.76
P(1)–C(16)	1.82 (3)	Mo(1)–H(1)	1.99
P(1)–C(22)	1.79 (3)	Mo(2)–H(1)	1.90
P(2)–C(9)	1.89 (3)		

Mo(2)–Au–P(1)	143.3 (2)	Au–P(1)–C(16)	114.3 (9)
Mo(1)–Au–P(1)	135.8 (2)	Au–P(1)–C(10)	110.9 (8)
Mo(1)–Au–Mo(2)	80.9 (1)	C(16)–P(1)–C(22)	105.0 (13)
Au–Mo(1)–C(4)	120.5 (9)	C(10)–P(1)–C(22)	107.3 (13)
Au–Mo(1)–C(3)	68.5 (7)	C(10)–P(1)–C(16)	107.9 (13)
Au–Mo(1)–C(2)	145.2 (10)	Mo(1)–P(2)–C(34)	111.2 (10)
Au–Mo(1)–C(1)	76.6 (7)	Mo(1)–P(2)–C(28)	117.4 (10)
Au–Mo(1)–P(2)	104.7 (2)	Mo(1)–P(2)–C(9)	118.8 (10)
C(2)–Mo(1)–C(4)	87.8 (14)	C(28)–P(2)–C(34)	101.5 (14)
C(2)–Mo(1)–C(3)	82.7 (12)	C(9)–P(2)–C(34)	101.7 (13)
C(1)–Mo(1)–C(4)	86.0 (13)	C(9)–P(2)–C(28)	103.9 (13)
C(1)–Mo(1)–C(3)	93.6 (12)	Mo(2)–P(3)–C(46)	120.4 (9)
C(1)–Mo(1)–C(2)	86.7 (13)	Mo(2)–P(3)–C(40)	109.7 (10)
P(2)–Mo(1)–C(4)	92.4 (9)	Mo(2)–P(3)–C(9)	113.5 (8)
P(2)–Mo(1)–C(3)	87.9 (8)	C(40)–P(3)–C(46)	104.1 (13)
P(2)–Mo(1)–C(2)	92.8 (8)	C(9)–P(3)–C(46)	106.7 (12)
Au–Mo(2)–C(8)	102.8 (10)	C(9)–P(3)–C(40)	100.1 (13)
Au–Mo(2)–C(7)	71.8 (7)	Mo(1)–C(1)–O(1)	173 (2)
Au–Mo(2)–C(6)	147.6 (9)	Mo(1)–C(2)–O(2)	172 (2)
Au–Mo(2)–C(5)	71.0 (8)	Mo(1)–C(3)–O(3)	176 (2)
Au–Mo(2)–P(3)	116.4 (2)	Mo(1)–C(4)–O(4)	169 (3)
C(6)–Mo(2)–C(8)	93.8 (14)	Mo(2)–C(5)–O(5)	168 (2)
C(6)–Mo(2)–C(7)	87.9 (12)	Mo(2)–C(6)–O(6)	177 (3)
C(5)–Mo(2)–C(8)	85.3 (14)	Mo(2)–C(7)–O(7)	179 (2)
C(5)–Mo(2)–C(7)	86.3 (11)	Mo(2)–C(8)–O(8)	165 (3)
C(5)–Mo(2)–C(6)	83.0 (11)	P(2)–C(9)–P(3)	115.9 (14)
P(3)–Mo(2)–C(8)	95.2 (11)	Mo(1)–H(1)–Mo(2)	153
P(3)–Mo(2)–C(7)	93.5 (8)	Au–H(1)–Mo(2)	106
P(3)–Mo(2)–C(6)	89.1 (9)	Au–H(1)–Mo(1)	101
Au–P(1)–C(22)	111.2 (10)		

Description of the X-ray Structure of $[Mo_2(CO)_8(\mu\text{-dppm})(\mu_3\text{-H})(\mu\text{-AuPPh}_3)]$ (1a). The structure of **1a** is depicted in Figure 2 together with the atomic numbering system; the most important bond distances and angles are given in Table I. The metal skeleton consists of an isosceles Mo_2Au triangle in which the two molybdenum atoms, at a very long distance of 3.771 (3) Å, are bridged by the dppm ligand through the two P atoms. The Mo–Au distances, 2.900 (3) and 2.914 (2) Å, although longer than those found in the complexes $[\{(PPh_3)Au\}_7Mo(CO)_3]OH$, in the range 2.771 (1)–2.860 (2) Å,[14] $[MoS_4(AuPPh_3)_2]$, 2.801 (1) and 2.818 (1) Å,[15] and $[MoS_4(AuPEt_3)_2]$, 2.815 (1) and 2.814 (1) Å,[16] suggest significant metal–metal interaction. The only Mo–Au bond distance longer than those found here has been reported for $[MoOS_3(AuPPh_3)\{(Au(PPh_3)_2\}]$, 2.838 (1) and 3.133 (1) Å.[16] The position of the hydride ligand, triply bridging the metal atoms and lying in the same plane defined by them, is

---

[12] Brown, S. S. D.; Salter, I. D.; Dent, A. J.; Kitchen, G. F. M.; Orpen, A. G.; Bates, P. A.; Hursthouse, M. B. *J. Chem. Soc., Dalton Trans.* **1989**, 1227.

[13] Reina, R.; Rossell, O.; Seco, M.; Perales, A. *J. Organomet. Chem.* **1991**, *415*, 101.

[14] Beuter, G.; Strähle, J. *Angew. Chem., Int. Ed. Engl.* **1988**, *27*, 1094.

[15] Charnock, J. M.; Bristow, S.; Nicholson, J. R.; Garner, C. D.; Clegg, W. *J. Chem. Soc., Dalton Trans.* **1987**, 303.

[16] Kinsch, E. M.; Stephan, D. W. *Inorg. Chim. Acta* **1985**, *96*, L87.

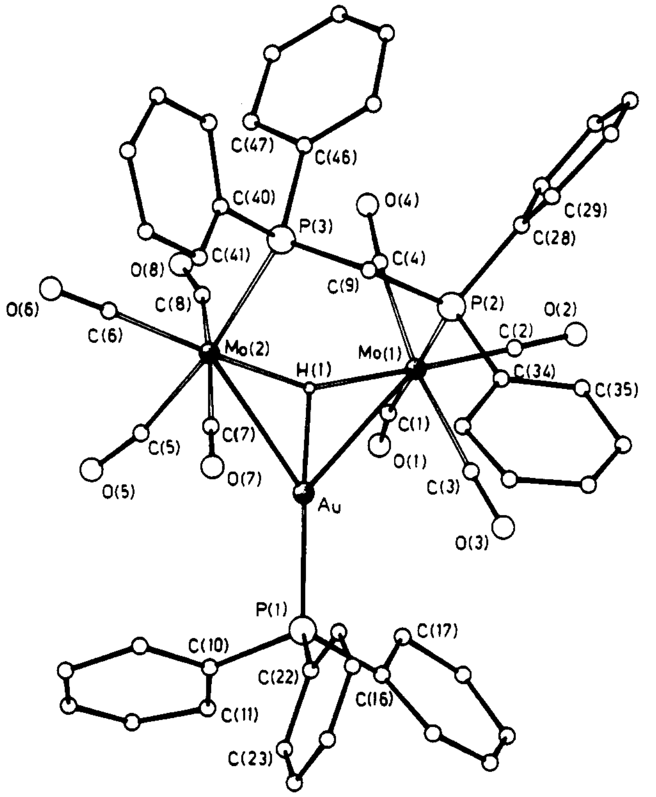

Figure 2. View of the molecular structure of $[(CO)_8Mo_2(\mu\text{-dppm})(\mu_3\text{-H})(\mu\text{-AuPPh}_3)]$ (**1a**) together with the atomic numbering scheme.

evidenced by several results (ligand orientation associated with the octahedral environment of the two Mo atoms, presence of a peak in the final ΔF map in this position, and also indirect location by means of a "potential-energy" technique and theoretical calculations). The Au–H bond length, 1.76 Å, compares well with the previously reported values in $[Au_2Ru(H)_2(dppm)_2(PPh_3)_2](NO_3)_2$, 1.77 (4) Å,[17] and in $[(OC)_5Cr(\mu\text{-H})(AuPR_3)]$, 1.72 (1) Å,[3] and is shorter than those reported for $[Au_2Ru_4(\mu_3\text{-H})(\mu\text{-H})(CO)_{12}(PPh_3)_2]$, 2.04 (10) Å,[7] $[AuRu(H)_2(dppm)_2(PPh_3)]\,PF_6$, 1.98 (6) Å,[18] and $Nb_3Au_3H_6(C_5H_4SiMe_3)_6]$, ≈1.88 Å.[19] The Mo–H bond lengths, 1.99 and 1.90 Å, are only slightly longer than those reported for the anion $[Mo_2(CO)_8(\mu\text{-dppm})(\mu\text{-H})]^-$, 1.89 (6) and 1.85 (6), Å,[11] and no report involving well-localized hydrides in μ_3-H molybdenum systems has been published. On the other hand, the Au–H–Mo angles, 101 and 106°, are comparable with other M–H–Au angles in the compounds $[(OC)_5Cr(\mu\text{-H})(AuPR_3)]$, 111 (5)°,[3] $[(PPh_3)Au(\mu\text{-H})Pt(C_6Cl_5)\,(PEt_3)_2](CF_3SO_3)$, 103 (4)°,[4a] and $[Au_2Ru_4(\mu_3\text{-H})(\mu\text{-H})(CO)_{12}(PPh_3)_2]$, 109 (4)°.[7]

A comparison of the most significant features of the structure of **1a** with respect to those of the starting anion $[Mo_2(CO)_8(\mu\text{-dppm})(\mu\text{-H})]^-$ [11] shows that the bonding of $[Au(PPh_3)]^+$ causes an elongation of the Mo–Mo separation, 3.771 (3) against 3.403 (1) Å, an opening of the Mo–H–Mo angle, 153 against 131 (3)°, and a slight lengthening of the Mo–P bond distances, 2.530 (7) and 2.557 (7) Å against 2.509 (2) and 2.513 (2) Å. Moreover if in **1a** the Mo–Au bonds are ignored, each Mo atom displays a roughly octahedral arrangement, involving four carbonyl groups, one P of the dppm ligand, and the hydride, comparable to that of the starting anion. Also the Mo–C bonds show the same trend: those of carbonyls trans to each other, in the range 2.03 (3)–2.04 (2) Å, are longer than those trans to either the P atom or the hydride, in the range 1.84 (3)–1.95 (3) Å.

Chart I

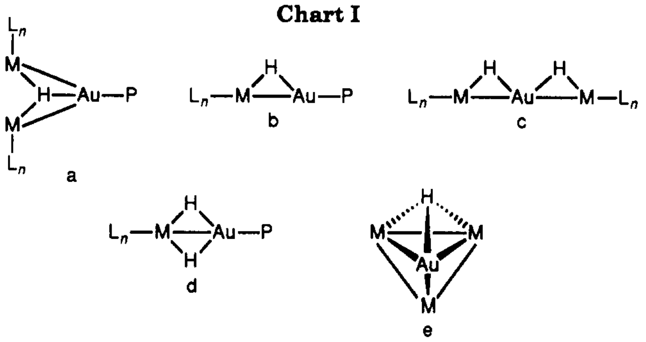

In conclusion, the structure of **1a**, exhibiting a hydride in the same plane defined by the three metals, represents a new structural type based on bonding interactions involving hydride complexes of gold–transition-metal clusters. Chart I includes all the structural situations described so far: (a) shows **1a** schematically; (b) represents the typical hydride which is bonding two metal centers simultaneously;[2-4] (c) shows two hydride atoms that are consecutively bridging three metal centers;[18,19,20,21] (d) shows two hydride atoms that are double-bridging two atoms;[18,22] (e) shows a hydride that is capping a face of a metal cluster.[7,12]

Electronic Structure and Bonding of 1a. The uniqueness of the bonding mode between the hydride and the three metals observed in **1a** deserves a closer examination of its electronic structure. Hence, a theoretical analysis of bonding in **1a** was carried out on the basis of extended Hückel molecular orbital calculations[23] and using standard atomic parameters from the literature.[24] The only simplification adopted in the model molecule used for the calculations was the substitution of the phenyl groups in the phosphine ligands by hydrogen atoms. The simplest way to study the bonding in the Mo_2HAu core consists in dissecting the molecule in two fragments and seeing how they interact. We have chosen to study the interaction between the fragments $[Mo_2(CO)_8(\mu\text{-dppm})(\mu\text{-H})]^-$ and $[AuPPh_3]^+$, which is *formally* analogous to the reaction actually employed in our synthetic procedure (eq 1). This approach will allow us to check the theoretical results with the structural differences between the *fragment* $[Mo_2(CO)_8(\mu\text{-dppm})(\mu\text{-H})]^-$ and the *molecule* $[Mo_2(CO)_8(\mu\text{-dppm})(\mu_3\text{-H})(\mu\text{-AuPPh}_3)]$. The orbital interaction between both fragments can be described schematically as in Figure 3. On the starting molybdenum compound we find the a_1 orbital, which is largely localized (70% of its electron density) on the hydride and responsible for the three

---

[17] Alexander, B. D.; Johnson, B. J.; Johnson, S. M.; Casalnuovo, A. L.; Pignolet, L. H. *J. Am. Chem. Soc.* **1986**, *108*, 4409.

[18] Alexander, B. D.; Johnson, B. J.; Johnson, S. M.; Boyle, P. D.; Kann, N. C.; Mueting, A. M.; Pignolet, L. H. *Inorg. Chem.* **1987**, *26*, 3506.

[19] Antiñolo, A.; Jalón, F. A.; Otero, A.; Fajardo, M.; Chaudret, B.; Lahoz, F.; López, J. A. *J. Chem. Soc., Dalton Trans.* **1991**, 1861.

[20] Albinati, A.; Demartin, F.; Venanzi, L. M.; Wolfer, M. K. *Angew. Chem., Int. Ed. Engl.* **1988**, *27*, 563.

[21] Alexander, B. D.; Gómez-Sal, M. P.; Gannon, P. R.; Blaine, C. A.; Boyle, P. D.; Mueting, A. M.; Pignolet, L. H. *Inorg. Chem.* **1988**, *27*, 3301.

[22] Alexander, B. D.; Boyle, P. D.; Johnson, B. J.; Casalnuovo, J. A.; Johnson, S. M.; Mueting, A. M.; Pignolet, L. H. *Inorg. Chem.* **1987**, *26*, 2547.

[23] (a) Hoffmann, R. *J. Chem. Phys.* **1963**, *39*, 1397. (b) Ammeter, J. H.; Bürgi, H.-B.; Thibeault, J. C.; Hoffmann, R. *J. Am. Chem. Soc.* **1978**, *100*, 3686.

[24] Atomic parameters for O and H see ref 23. P: Summerville, R. H.; Hoffmann, R. *J. Am. Chem. Soc.* **1976**, *98*, 7240. Mo: Summerville, R. H.; Hoffmann, R. *J. Am. Chem. Soc.* **1976**, *98*, 7240. Au: Komiya, S.; Albright, T. A.; Hoffmann, R.; Kochi, J. K. *J. Am. Chem. Soc.* **1977**, *99*, 8440.

Table II. Calculated Overlap Populations within the Mo_2H and Mo_2HAu Frameworks in $[Mo_2(\mu\text{-dppm})(\mu\text{-H})(CO)_8]^-$[11] and $[(CO)_8Mo_2(\mu\text{-dppm})(\mu_3\text{-H})(\mu\text{-AuPPh}_3)]$ (1a), Respectively, with Experimental Bond Distances in Parentheses (Å)

bond	Mo_2H	Mo_2HAu
Mo(1)-H	0.296 (1.89)	0.199 (1.99)
Mo(2)-H	0.310 (1.85)	0.210 (1.90)
Mo(1)-Mo(2)	0.025 (3.40)	0.015 (3.77)
Mo(1)-Au		0.087 (2.90)
Mo(2)-Au		0.091 (2.91)
Au-H		0.290 (1.76)

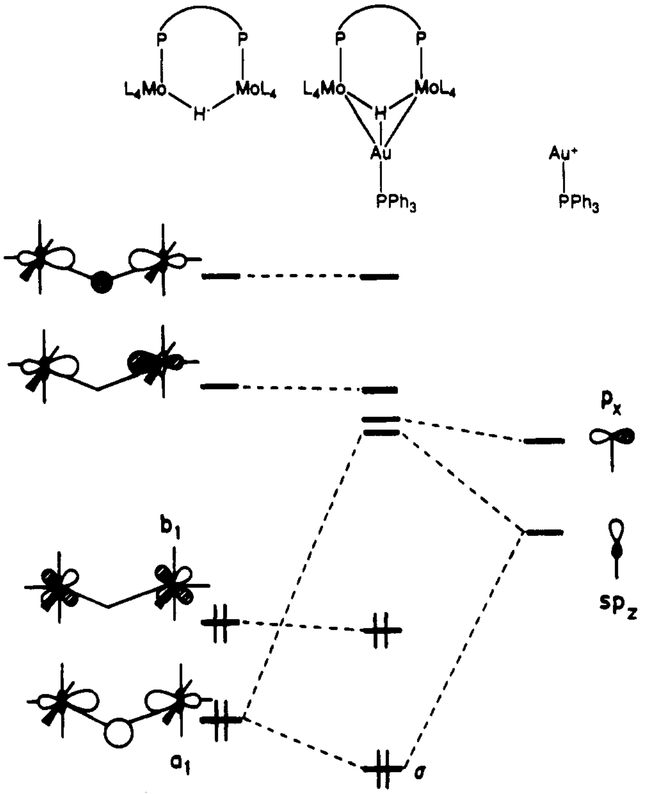

Figure 3. Diagram of the orbital interaction between $[Mo_2(CO)_8(\mu\text{-dppm})(\mu\text{-H})]^-$ and $AuPPh_3{}^+$.

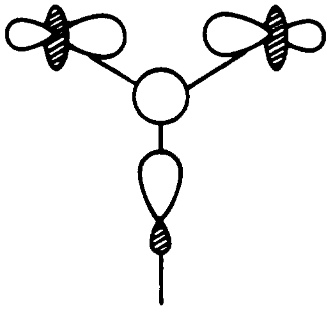

Figure 4. Schematic representation of the σ orbital of **1a**.

center–two electron bond of the Mo_2H group.[25] The hydride character of the hydrogen atom can be seen in its calculated net charge (−0.39). The a_1 orbital is strongly stabilized through interaction with the empty sp_z lobe of $[AuPPh_3]^+$, as indicated by the calculated overlap population of 0.458 between those orbitals. Thus, the resulting molecular orbital (labeled σ in Figure 3 and schematically represented in Figure 4) has σ-bonding character between each pair of atoms of the Mo_2HAu group, but the hydrogen atom retains most of its hydride character, its calculated net charge being −0.25. There is also some interaction of the b_1 combination of t_{2g}-like orbitals of the Mo atoms with the p_x orbital of Au (overlap population 0.071) but it is much less important than that between a_1 orbitals and, consequently, one can conclude that the Mo_2HAu skeleton is held together essentially by means of the molecular orbital depicted in Figure 4.

This very simple bonding scheme has a number of implications worthy of discussion. (i) The donation of electron density from a_1 of $[Mo_2(CO)_8(\mu\text{-dppm})(\mu\text{-H})]^-$ to sp_z of $[AuPPh_3]^+$ produces a weakening of the Mo–H bonding interaction. The decrease in the average of the calculated Mo–H overlap populations (see Table II) upon bonding to $[AuPPh_3]^+$ (from 0.303 to 0.204) is consistent with changes in the averages of the bond distances (from 1.87[11] to 1.94 Å). (ii) Although there is no *true* bond between the two Mo atoms in $[Mo_2(CO)_8(\mu\text{-dppm})(\mu\text{-H})]^-$, there may be a small bonding interaction according to the small positive overlap population calculated, which is made smaller after interacting with $[AuPPh_3]^+$ (see Table II). This variation can be detected in the structural data both in the nonbonded Mo–Mo distances (Table II) and in the increased Mo–H–Mo bond angle: 131° for $[Mo_2(CO)_8(\mu\text{-dppm})(\mu\text{-H})]^-$ and 153° for $[Mo_2(CO)_8(\mu\text{-dppm})(\mu_3\text{-H})(\mu\text{-AuPPh}_3)]$. (iii) A bonding interaction between the Mo and Au atoms should also be present, according to the topology of the orbital shown in Figure 4 and the calculated overlap populations (Table II). The relatively short Mo–Au distances (2.90 and 2.91 Å, as compared to the typical distances for Mo–Au bonds, 2.7–2.8 Å) and the increased Mo–H–Mo angle are consistent with the existence of weak, bonding Mo–Au interactions. (iv) The molecule of $[Mo_2(CO)_8(\mu\text{-dppm})(\mu_3\text{-H})(\mu\text{-AuPPh}_3)]$ offers a rare example of a four center–two electron bond in which a bridging hydride holds three metal atoms together. The description of the bonding in **1a** suggests that the hydride abstraction reaction should result in the falling apart of the trimetallic framework although we have seen that **1a** is recovered unaltered after treatment of its tetrahydrofuran solutions with a large excess of trifluoroacetic acid. (v) The interaction of the hydride with the orbitals of the metal atoms is optimum when it sits in the plane of the Mo_2Au triangle in sharp contrast with the case of hydride-bridged trimetallic clusters with metal–metal bonds, in which the hydride is out of the plane.[26] A restricted geometrical optimization indicates that the most stable position for the hydride ligand is in the plane of the Mo_2Au skeleton and equidistant to both Mo atoms, with a flat potential well around the minimum, in good agreement with its localization from the diffraction data.

Experimental Section

All manipulations were performed under an atmosphere of prepurified N_2 with use of standard Schlenk techniques, and all solvents were distilled from appropriate drying agents. Elemental analyses of C and H were carried out at the Institut de Bio-Orgànica de Barcelona. Infrared spectra were recorded in THF solutions on a Perkin-Elmer 1330 spectrophotometer. $^{31}P\{^1H\}$ NMR spectra were obtained on a Bruker WP 80SY spectrometer (δ(85% H_3PO_4) = 0.0 ppm). ^1H NMR were obtained on Bruker

---

(25) Albright, T. A.; Burdett, J. K.; Whangbo, M.-H. *Orbital Interactions in Chemistry*; J. Wiley: New York, 1985; p 328.

(26) Cotton, F. A.; Poli, R. *J. Am. Chem. Soc.* **1988**, *110*, 830.

Table III. Summary of Crystallographic Data for Complex 1a

mol formula	$C_{51}H_{38}AuMo_2O_8P_3$	V, Å^3	4841 (3)
mol wt	1260.62	Z	4
cryst syst	orthorhombic	D_{calcd}, g cm^{-3}	1.730
space group	$P2_12_12_1$	$F(000)$	2464
a, Å	12.361 (5)	μ(Mo Kα), cm^{-1}	36.65
b, Å	15.179 (6)	R	0.0504
c, Å	25.800 (8)	R_w	0.0668

WP 80SY, Varian XL-200, and Varian XL-500 spectrometers (δ(TMS) = 0.00 ppm). $ClAuPPh_3$,[27] $IAgPPh_3$,[28] and $ICuPPh_3$[29] were prepared as described previously. The complexes $(ClAu)_2(\mu\text{-dppm})$, $(ClAu)_2(\mu\text{-dppe})$, and $(ClAu)_2(\mu\text{-dppp})$ were synthesized and isolated as solids from ClAu(tht)[30] solutions by adding the appropriate amount of the corresponding diphosphine.

Synthesis of $[Mo_2(CO)_8(\mu\text{-dppm})(\mu_3\text{-H})(\mu\text{-AuPPh}_3)]$ (1a). To a previously cooled (−20 °C) THF (20 mL) solution of $(NEt_4)[Mo_2(CO)_8(\mu\text{-dppm})(\mu\text{-H})]$ (0.400 g, 0.43 mmol) were added 0.215 g (0.43 mmol) of $ClAuPPh_3$ and 0.125 g (0.43 mmol) of $TlBF_4$. After 10 min of stirring at 0 °C, the mixture was filtered to eliminate NEt_4BF_4 and TlCl salts and the yellow solution was evaporated to dryness. The resulting solid was extracted with precooled (−20 °C) toluene (2 × 5 mL). Subsequent addition of hexane (20 mL) afforded the analytically pure compound as orange microcrystals: yield 0.38 g (70%); IR (THF, cm^{-1}) ν(CO) stretch 2020 m, 2000 s, 1950 m, 1925 vs, 1890 vs, 1870 m; $^{31}P\{^1H\}$ NMR (−20 °C, THF, δ (ppm)) 48.9 (t, *P*Au, ^3J(P–P) = 6.8 Hz), 29.7 (d, *P*Mo, ^3J(P–P) = 6.8 Hz); ^1H NMR (25 °C, acetone-d_6, δ (ppm)) −10.66 (d of t, 1 H, μ_3-H, $^2J(P_{Au}\text{–H})$ = 85.9 Hz, $^2J(P_{Mo}\text{–H})$ = 10.4 Hz), 3.75 (t, 2 H, PCH_2P, ^2J(P–H) = 9.7 Hz), 7.22–7.64 (m, 35 H, Ph). Anal. Calcd for $C_{51}H_{38}AuMo_2O_8P_3$: C, 48.58; H, 3.02. Found: C, 48.65; H, 3.10.

Synthesis of $[Mo_2(CO)_8(\mu\text{-dppm})(\mu_3\text{-H})(\mu\text{-MPPh}_3)]$ [M = Ag (1b), Cu (1c)]. To a previously cooled (−20 °C) THF (20 mL) solution of $(NEt_4)[Mo_2(CO)_8(\mu\text{-dppm})(\mu\text{-H})]$ (0.400 g, 0.43 mmol) was added 0.195 g (0.43 mmol) of $ICuPPh_3$ and 0.125 g (0.43 mmol) of $TlBF_4$. After 10 min of stirring at 0 °C, the mixture was filtered to eliminate NEt_4BF_4 and TlI salts and the pale yellow solution was evaporated to dryness. The resulting solid was extracted with precooled (−20 °C) toluene (2 × 5 mL). Subsequent addition of hexane (20 mL) afforded the analytically pure compound as bright yellow microcrystals: yield 0.35 g (72%); IR (THF, cm^{-1}) ν(CO) stretch 2020 m, 1995 s, 1950 m, 1925 vs, 1900 vs, 1865 vs; $^{31}P\{^1H\}$ NMR (−20 °C, THF, δ (ppm)) 27.4 (d, *P*Mo, ^3J(P–P) = 4.2 Hz), 5.3 (t, *P*Cu, ^3J(P–P) = 4.2 Hz); ^1H NMR (25 °C, C_6D_6, δ (ppm)) −13.32 (d of t, 1 H, μ_3-H, $^2J(P_{Cu}\text{–H})$ = 29.8 Hz, $^2J(P_{Mo}\text{–H})$ = 10.7 Hz), 3.56 (t, 2 H, PCH_2P, ^2J(P–H) = 9.3 Hz), 6.87–7.80 (m, Ph). Anal. Calcd for $C_{51}H_{38}CuMo_2O_8P_3$: C, 54.34; H, 3.40. Found: C, 54.38; H, 3.49.

A similar procedure was used to prepare the silver derivative **1b**. To avoid a silver deposition reaction, mixtures were protected from light: yield 0.34 g (68%); IR (THF, cm^{-1}) ν(CO) stretch 2015 m, 1995 s, 1950 m, 1920 vs, 1895 vs, 1870 vs; $^{31}P\{^1H\}$ NMR (−20 °C, THF, δ (ppm)) 27.6 (s (broad), *P*Mo, ^3J(P–P) = not observable), 14.7 (2 × d of t, *P*Ag, $^1J(P\text{–}^{107}Ag)$ = 483 Hz, $^1J(P\text{–}^{109}Ag)$ = 556 Hz); ^1H NMR (25 °C, C_6D_6, δ (ppm)) −12.14 (d of m (broad), 1 H, μ_3-H, $^1J(H\text{–}^{107}Ag)$, $^1J(H\text{–}^{109}Ag)$ = not observable), 3.54 (t, 2 H, PCH_2P, ^2J(P–H) = 9.2 Hz, 6.88–7.67 (m, Ph). Anal. Calcd for $C_{51}H_{38}AgMo_2O_8P_3$: C, 52.29; H, 3.27. Found: C, 52.33; H, 3.31.

Synthesis of $[\{(CO)_8Mo_2(\mu\text{-dppm})(\mu_3\text{-H})(\mu\text{-Au})\}_2(PP)]$ [PP = dppm (2a), dppp (2c)]. To a previously cooled (−20 °C) THF (20 mL) solution of $(NEt_4)[Mo_2(CO)_8(\mu\text{-dppm})(\mu\text{-H})]$ (0.410 g, 0.44 mmol) was added 0.187 g (0.22 mmol) of $(ClAu)_2$dppm and 0.128 g (0.44 mmol) of $TlBF_4$. After 10 min of stirring at 0 °C, the mixture was filtered to eliminate NEt_4BF_4 and TlCl salts and the orange solution was evaporated to dryness. The resulting solid was extracted with precooled (−20 °C) toluene (2 × 5 mL). Subsequent addition of hexane (20 mL) afforded the analytically pure compound as orange microcrystals: yield 0.38 g (72%); IR (THF, cm^{-1}) ν(CO) stretch 2010 m, 2000 s, 1950 s, 1920 vs, 1900 vs, 1870 vs; $^{31}P\{^1H\}$ NMR (−20 °C, THF, δ (ppm)) 40.7 (s (broad), *P*Au, ^3J(P–P) = not observable), 28.6 (s (broad), *P*Mo); ^1H NMR (25 °C, C_6D_6, δ (ppm)) −11.42 (d of t, 2 H, μ_3-H, $^2J(P_{Au}\text{–H})$ = 87.9 Hz, $^2J(P_{Mo}\text{–H})$ = 8.2 Hz), 3.56 (t, 4 H, $MoPCH_2PMo$, ^2J(P–H) = 9.2 Hz), 4.56 (t, 2 H, $AuPCH_2PAu$, ^2J(P–H) = 9.8 Hz), 7.02–7.93

Table IV. Fractional Atomic Coordinates (×10^4) and Isotropic Thermal Parameters (Å^2 × 10^4) with Esd's in Parentheses for the Non-Hydrogen Atoms of 1a

atom	x/a	y/b	z/c	U
Au	4385 (1)	3765 (1)	1180 (1)	420 (3)[a]
Mo(1)	3400 (2)	5190 (2)	599 (1)	391 (8)[a]
Mo(2)	2333 (2)	3883 (2)	1732 (1)	366 (7)[a]
P(1)	5998 (5)	3029 (5)	1157 (4)	471 (24)[a]
P(2)	3317 (5)	6464 (4)	1230 (3)	394 (21)[a]
P(3)	1619 (6)	5435 (4)	1911 (3)	377 (23)[a]
O(1)	3530 (21)	3669 (18)	−218 (9)	808 (96)[a]
O(2)	3574 (22)	6334 (17)	−383 (10)	941 (107)[a]
O(3)	5951 (16)	5372 (14)	598 (10)	685 (89)[a]
O(4)	894 (20)	5228 (20)	327 (11)	942 (115)[a]
O(5)	2808 (16)	1890 (14)	1671 (10)	697 (90)[a]
O(6)	921 (17)	3181 (16)	2633 (9)	717 (87)[a]
O(7)	4225 (16)	4050 (14)	2539 (8)	622 (78)[a]
O(8)	562 (24)	3315 (20)	937 (14)	1279 (141)[a]
C(1)	3421 (25)	4224 (16)	108 (11)	425 (96)[a]
C(2)	3539 (26)	5924 (17)	36 (13)	529 (106)[a]
C(3)	5046 (20)	5303 (19)	615 (10)	381 (92)[a]
C(4)	1774 (28)	5217 (21)	480 (12)	539 (116)[a]
C(5)	2745 (24)	2648 (16)	1672 (9)	451 (95)[a]
C(6)	1417 (24)	3440 (18)	2290 (14)	563 (115)[a]
C(7)	3550 (21)	3989 (18)	2258 (10)	419 (93)[a]
C(8)	1233 (27)	3604 (31)	1171 (14)	933 (174)[a]
C(9)	2665 (18)	6285 (22)	1885 (10)	472 (91)[a]
C(10)	5789 (20)	1835 (17)	1229 (11)	446 (66)
C(11)	6013 (22)	1245 (22)	825 (11)	583 (76)
C(12)	5662 (28)	376 (23)	891 (15)	739 (94)
C(13)	5272 (28)	142 (27)	1355 (14)	756 (108)
C(14)	5077 (29)	640 (25)	1759 (16)	806 (107)
C(15)	5297 (21)	1562 (18)	1691 (11)	471 (71)
C(16)	6778 (21)	3209 (17)	570 (11)	404 (65)
C(17)	6175 (26)	3208 (20)	76 (12)	572 (81)
C(18)	6808 (26)	3310 (21)	−358 (12)	606 (85)
C(19)	7891 (24)	3518 (21)	−344 (13)	591 (86)
C(20)	8358 (26)	3571 (20)	101 (12)	566 (82)
C(21)	7861 (24)	3472 (20)	561 (13)	609 (85)
C(22)	6869 (23)	3374 (19)	1674 (12)	483 (73)
C(23)	7717 (21)	2804 (19)	1839 (11)	452 (69)
C(24)	8444 (32)	3089 (25)	2223 (15)	796 (107)
C(25)	8332 (29)	3909 (25)	2463 (14)	769 (104)
C(26)	7532 (30)	4432 (26)	2296 (15)	821 (113)
C(27)	6790 (27)	4121 (22)	1928 (13)	642 (91)
C(28)	2722 (23)	7485 (19)	1001 (11)	485 (73)
C(29)	2796 (28)	8252 (23)	1304 (15)	741 (101)
C(30)	2371 (27)	9092 (24)	1114 (15)	785 (102)
C(31)	1836 (29)	9083 (27)	657 (16)	876 (118)
C(32)	1657 (31)	8293 (23)	358 (14)	774 (104)
C(33)	2139 (24)	7547 (22)	572 (13)	601 (86)
C(34)	4665 (25)	6825 (21)	1412 (12)	580 (89)
C(35)	5187 (23)	7424 (21)	1087 (12)	580 (81)
C(36)	6269 (26)	7729 (23)	1220 (15)	716 (93)
C(37)	6725 (29)	7465 (24)	1607 (14)	776 (105)
C(38)	6257 (33)	6863 (26)	1932 (17)	919 (127)
C(39)	5206 (28)	6508 (24)	1835 (15)	771 (107)
C(40)	1208 (23)	5527 (20)	2605 (12)	490 (74)
C(41)	1881 (23)	5341 (19)	2968 (11)	510 (74)
C(42)	1499 (24)	5328 (20)	3491 (11)	538 (80)
C(43)	459 (25)	5633 (20)	3605 (12)	583 (83)
C(44)	−213 (27)	5926 (21)	3228 (14)	691 (94)
C(45)	166 (22)	5902 (17)	2695 (11)	447 (71)
C(46)	442 (22)	5867 (18)	1549 (11)	437 (72)
C(47)	−343 (22)	5249 (20)	1398 (11)	501 (76)
C(48)	−1185 (27)	5577 (22)	1104 (14)	686 (94)
C(49)	−1240 (30)	6427 (26)	964 (15)	843 (112)
C(50)	−513 (32)	7051 (28)	1146 (16)	950 (118)
C(51)	417 (28)	6791 (22)	1436 (13)	634 (96)

[a] Equivalent isotropic U defined as one-third of the trace of the orthogonalized $\mathbf{U}_{ij}$ tensor.

---

(27) Kowala, C.; Swan, J. M. *Aust. J. Chem.* **1966**, *19*, 547.
(28) Teo, B. K.; Calabrese, J. *Inorg. Chem.* **1976**, *15*, 2474.
(29) Kauffman, B. B.; Teter, L. A. *Inorg. Synth.* **1963**, *7*, 9.
(30) Usón, R.; Laguna, A. *Organomet. Synth.* **1986**, *3*, 324.

(m, Ph). Anal. Calcd for $C_{91}H_{68}Au_2Mo_4O_{16}P_6$: C, 45.90; H, 2.88. Found: C, 45.96; H, 3.03.

The **2c** derivative was prepared in a similar manner: yield 0.41 g (77%); IR (THF, cm^{-1}) ν(CO) stretch 2015 m, 1995 m, 1950 s, 1925 vs, 1895 vs, 1875 vs, $^{31}P\{^1H\}$ NMR (−20 °C, THF, δ (ppm)) 43.7 (t, *P*Au, ^3J(P–P) = 5.8 Hz), 31.1 (d, *P*Mo, ^3J(P–P) = 5.8 Hz); ^1H NMR (25 °C, C_6D_6, δ (ppm)) −10.53 (d of t, 2 H, μ_3-H, ^2J(P_{Au}–H) = 84.5 Hz, ^2J(P_{Mo}–H) = 10.1 Hz), 2.21 (m, 2 H, $AuPCH_2CH_2CH_2PAu$), 2.66 (m, 4 H, $AuPCH_2CH_2CH_2PAu$), 3.53 (t, 4 H, $MoPCH_2PMo$, ^2J(P–H) = 9.4 Hz), 6.84–7.77 (m, Ph). Anal. Calcd for $C_{93}H_{72}Au_2Mo_4O_{16}P_6$: C, 46.37; H, 3.01. Found: C, 46.39; H, 2.99.

Synthesis of [{$Mo_2(CO)_8$(μ-dppm)(μ_3-H)(μ-Au)}$_2$(PP)] [PP = dppe (2b)]. To a previously cooled (−20 °C) THF (20 mL) solution of $(NEt_4)[(CO)_8Mo_2(\mu\text{-dppm})(\mu\text{-H})]$ (0.410 g, 0.44 mmol) was added 0.190 g (0.22 mmol) of $(ClAu)_2$dppe and 0.128 g (0.44 mmol) of $TlBF_4$. After 10 min of stirring at 0 °C, the mixture was filtered to eliminate NEt_4BF_4 and TlCl salts and the orange solution was evaporated to dryness. The solid residue can be recrystallized from a THF/hexane mixture giving the pure compound as yellow microcrystals: yield 0.38 g (72%); IR (THF, cm^{-1}) ν(CO) stretch 2015 m, 1995 m, 1950 s, 1925 vs, 1900 vs, 1880 vs; $^{31}P\{^1H\}$ NMR (−20 °C, THF, δ (ppm)) 47.9 (s (broad), *P*Au, ^3J(P–P) = not observable), 29.9 (s (broad), *P*Mo); ^1H NMR (25 °C, C_6D_6, δ (ppm)) −10.30 (d of t, 2 H, μ_3-H, ^2J(P_{Au}–H) = 84.2 Hz, ^2J(P_{Mo}–H) = 10.4 Hz), 3.41 (m, 4 H, $AuPCH_2CH_2PAu$), 3.57 (t, 4 H, $MoPCH_2PMo$, ^2J(P–H) = 7.6 Hz), 6.89–7.98 (m, Ph). Anal. Calcd for $C_{92}H_{70}Au_2Mo_4O_{16}P_6$: C, 46.14; H, 2.94. Found: C, 46.21; H, 3.02.

X-ray Data Collection, Structure Determination, and Refinement for [$Mo_2(CO)_8$(μ-dppm)(μ_3-H)(μ-$AuPPh_3$)] (1a). A single crystal ca. 0.23 × 0.25 × 0.30 mm was selected and used for data collection. The crystallographic data are summarized in Table III. Unit cell parameters were determined from the θ values of 30 carefully centered reflections, having $11 < \theta < 17°$. Data were collected at room temperature on a Siemens AED diffractometer, using the niobium-filtered Mo Kα radiation (λ = 0.710 73 Å) and the $\theta/2\theta$ scan type. The reflections were collected with a variable scan speed of 3–12° min^{-1} and a scan width from $(\theta - 0.60)°$ to $(\theta + 0.60 + 0.346 \tan\theta)°$. Of 4765 unique reflections, with θ in the range 3–25°, 2309 with $I \geq 2\sigma(I)$ were used for the analysis. One standard reflection was monitored every 50 measurements; no significant decay was noticed over the time of data collection. The individual profiles have been analyzed following Lehmann and Larsen.[31] Intensities were corrected for Lorentz and polarization effects. A correction for absorption was applied (maximum and minimum values for the transmission factors were 1.167 and 0.869).[32]

The structure was solved by Patterson and Fourier methods and refined by full-matrix least-squares first with isotropic thermal parameters and then with anisotropic thermal parameters for all non-hydrogen atoms excepting the carbon atoms of the phenyl groups. Since the space group $P2_12_12_1$ leads to a chiral configuration in the structure, an independent final cycle of refinement was carried out using the coordinates $-x, -y, -z$ for the non-hydrogen atoms. A remarkable increase of the R values was obtained [$R(x, y, z) = 0.0546$; $R(-x, -y, -z) = 0.0827$]. The former model was selected, and the reported data refer to this model. All hydrogen atoms, excepting the hydride, were placed at their geometrically calculated positions (C–H = 1.00 Å) and refined "riding" on the corresponding carbon atoms. As regards the hydride, even if in the X-ray structure, determined at room temperature and in the presence of a heavy atom like gold, an accurate location was not found, a peak in the expected position (triply bridging the metals) was found in the final ΔF map. As expected, the refinement of the positional parameters did not give good results, so the found coordinates in fixed positions were introduced in the final calculations, and only the isotropic thermal parameter was refined. The position of the hydride was calculated also by minimization of the potential energy of the intramolecular nonbonded interactions involving the hydride by using the HYDEX program,[33] and its was quite in agreement with that found in the final ΔF map. The final cycles of refinement were carried out on the basis of 381 variables; after the last cycles, no parameters shifted by more than 0.50 times their esd. The biggest remaining peak (close to the gold atom) in the final difference map was equivalent to about 0.75 e/Å^3. In the final cycles of refinement a weighting scheme, $w = K[\sigma^2(F_o) + gF_o^2]^{-1}$ was used; at convergence the K and g values were 0.3747 and 0.0205, respectively. The analytical scattering factors, corrected for the real and imaginary parts of anomalous dispersions, were taken from ref 34. All calculations were carried out on the CRAY X-MP/48 computer of the "Centro di Calcolo Elettronico Interuniversitario dell'Italia Nord-Orientale" (CINECA, Casalecchio Bologna, Italy) and on the Gould Powernode 6040 of the "Centro di Studio per la Strutturistica Diffrattometrica" del CNR Parma, Italy, using the SHELX-76 and SHELXS-86 systems of crystallographic computer programs.[35] The final atomic coordinates for the non-hydrogen atoms are given in Table IV. The atomic coordinates of the hydrogen atoms are given in Table SI, and the thermal parameters, in Table SII.

Acknowledgment. Financial support for this work was generously given by the DGICYT (Spain), through Grants PB90-0055-C02-01 (experimental work) and PB89-0268 (theoretical studies).

Supplementary Material Available: Tables of hydrogen atom coordinates (Table SI), anisotropic thermal parameters for the non-hydrogen atoms (Table SII), and complete bond distances and angles (Table SIII) (7 pages). Ordering information is given on any current masthead page.

OM920138T

---

(31) Lehmann, M. S.; Larsen, F. K. *Acta Crystallogr., Sect. A* **1974**, *30*, 580.

(32) Walker, N.; Stuart, D. *Acta Crystallogr., Sect. A* **1983**, *39*, 158. Ugozzoli, F. *Comput. Chem.* **1987**, *11*, 109.

(33) Orpen, A. G. *J. Chem. Soc., Dalton Trans.* **1980**, 2509.

(34) *International Tables for X-Ray Crystallography*; Kynoch Press: Birmingham, England, 1974; Vol. IV.

(35) Sheldrick, G. M. SHELX-76 Program for crystal structure determination. University of Cambridge, England, 1976. Sheldrick, G. M. SHELXS-86 Program for the solution of crystal structures. University of Göttingen, 1986.